Beam Alignment for the Cell-Free mmWave Massive MU-MIMO Uplink

Jannik Brun, Victoria Palhares, Gian Marti, and Christoph Studer

Department of Information Technology and Electrical Engineering, ETH Zurich, Zurich, Switzerland
e-mail: brunj@student.ethz.ch, vmenescal@ethz.ch, gimarti@ethz.ch, studer@ethz.ch

Abstract—**Millimeter-wave (mmWave) cell-free massive multi-user (MU) multiple-input multiple-output (MIMO) systems combine the large bandwidths available at mmWave frequencies with the improved coverage of cell-free systems. However, to combat the high path loss at mmWave frequencies, user equipments (UEs) must form beams in meaningful directions, i.e., to a nearby access point (AP). At the same time, multiple UEs should avoid transmitting to the same AP to reduce MU interference. We propose an interference-aware method for beam alignment (BA) in the cell-free mmWave massive MU-MIMO uplink. In the considered scenario, the APs perform full digital receive beamforming while the UEs perform analog transmit beamforming. We evaluate our method using realistic mmWave channels from a commercial ray-tracer, showing the superiority of the proposed method over omnidirectional transmission as well as over methods that do not take MU interference into account.**

I. INTRODUCTION

Millimeter-wave (mmWave) cell-free massive multi-user (MU) multiple-input multiple-output (MIMO) is expected to be a key to reliable high-throughput wireless connectivity: mmWave frequencies provide large portions of contiguous bandwidth [1] and cell-free systems promise improved coverage even under the notoriously challenging propagation characteristics at mmWave frequencies [2]. However, these advantages come at the prize of formidable engineering challenges. mmWave communication has thus been an active research topic for a number of years [1], [3], [4] and recently found its way into commercial products [5]. While cell-free massive MU-MIMO has also been an area of active research [6]–[8], the bulk of studies has been devoted to sub-6-GHz communication and typically assumes single-antenna transceivers both for the user equipments (UEs) as well as for the access points (APs) [6]–[8].

Even in the mmWave cell-free literature, the UEs are often assumed to have a single antenna only [9]–[14], or, if they have multiple antennas, they do not perform any kind of beamforming with these [2], [15] (with the exception of [16]). However, the high path loss at mmWave frequencies is expected to require UE-side beamforming even in cell-free systems: Rather than aimlessly transmitting the uplink signal in all directions, a UE should form a beam that is aligned to a nearby AP. The challenge of determining the optimal beam

direction in which a UE should transmit is exacerbated by the fact that multiple UEs should avoid transmitting to the same (few-antenna) AP to mitigate MU interference.

A. Contributions

We consider the problem of beam alignment (BA) in the uplink of cell-free mmWave massive MU-MIMO systems. In the considered scenario, the UEs are able to perform analog beamforming and the APs of the cell-free system are able to perform digital beamforming. In contrast to what is customary in the cell-free literature, we do not assume that the number of APs is much larger than the number of UEs served [17], as such an assumption depends on a high pervasiveness of wireless infrastructure. We propose a MU interference-aware method for BA in the cell-free mmWave massive MU-MIMO uplink. The proposed method is complemented with an efficient block-sparse channel estimation (CHEST) method and a centralized linear minimum mean square error (LMMSE) equalizer. The resulting scheme is evaluated using realistic mmWave channels from a commercial ray-tracer [18], and with realistic transmit powers and noise figures. Our results show that omnidirectional transmission at the UEs leads to inferior performance compared to the proposed scheme. In ablation studies we show that the limited capabilities of the UEs compared to fully digital beamforming seem to be of little importance, whereas the interference-awareness of the BA algorithm contributes significantly to performance. These findings suggest that the problem of BA in dense cell-free mmWave networks should be considered from a global perspective while the precise radio-frequency (RF) architecture of the UEs is comparably less important.

B. Relevant Prior Art

Although there exists a substantial body of literature on cell-free systems with mmWave frequencies [2], [9]–[16], most of these works do either not consider beamforming at all [9], or they consider beamforming only at the APs [2], [10]–[15]. References [11]–[14] consider APs with different variants of hybrid beamforming and single-antenna UEs, while [10] considers APs with analog beamforming and single-antenna UEs. References [2], [15] assume APs with hybrid beamforming and multi-antenna UEs, but the UEs do not use beamforming (the multiple antennas are only used for increased array gain). To our

knowledge, the only existing work that considers the problem of beamforming or beam alignment on the UE side is [16], which proposes a scheme in which the UEs simultaneously estimate the direction of arrival (and departure) of the strongest beam. This paper also devises an algorithm that partitions the APs into sets to minimize the interference between APs which use non-orthogonal transmit patterns.

In stark contrast with previous work, we propose an interference-aware UE BA method for the uplink of cell-free mmWave massive MU-MIMO systems that takes multi-antenna APs and UEs into account. Unlike other works, we consider a scenario in which there are more UEs than APs in the same time-frequency resource, which is of practical importance. Additionally, in opposition to the largely assumed hybrid architectures, we study the situation where UEs rely on analog beamforming and APs are fully digital [19].

C. Notation

Upper case and lower case bold symbols denote matrices and vectors, respectively. The $N \times N$ identity matrix is given by $\mathbf{I}_N$. $\mathbf{A}^T$ and $\mathbf{A}^H$ are the transpose and conjugate transpose of $\mathbf{A}$, respectively; and $\mathbf{A}_{l,k}$ is the matrix in the lth row block and kth column block of the matrix $\mathbf{A}$. $\mathrm{diag}(\mathbf{a}_1, \ldots, \mathbf{a}_N)$ is a block-diagonal matrix whose diagonal blocks are $\mathbf{a}_1, \ldots, \mathbf{a}_N$. The Euclidean and Frobenius norms are $\|\cdot\|_2$ and $\|\cdot\|_F$, respectively.

II. SYSTEM MODEL

We consider the uplink of a cell-free mmWave massive MU-MIMO system with L locally distributed APs that are connected to a central processing unit (CPU) and jointly serve K UEs, see Fig. 1. Such a scenario could correspond for instance to a shopping mall or a university campus. The APs and UEs each have n_{AP} and n_{UE} antennas respectively, so that the total number of receive and transmit antennas is $N_R = n_{\mathrm{AP}}L$ and $N_T = n_{\mathrm{UE}}K$, respectively. The UEs are assumed to have a single RF chain and thus rely on analog beamforming; the APs are assumed to be fully digital, i.e., every antenna is connected to its own RF chain.[1]

We assume a frequency-selective mmWave channel which is divided into n_{sc} frequency-flat subcarriers using orthogonal frequency-division multiplexing (OFDM). The per-subcarrier input-output relation between all UEs and APs is expressed as

$$\mathbf{y} = \mathbf{HPs} + \mathbf{n}, \tag{1}$$

where we omit the subcarrier index for ease of notation. Here, $\mathbf{y} \in \mathbb{C}^{N_R}$ is the receive vector, $\mathbf{H} \in \mathbb{C}^{N_R \times N_T}$ is the channel matrix, $\mathbf{P} \in \mathbb{C}^{N_T \times K}$ is the UE beamforming matrix, $\mathbf{s} \in \mathbb{C}^K$ is the vector of UE transmit symbols with per-symbol energy E_s, and $\mathbf{n} \in \mathbb{C}^{N_R}$ is i.i.d. circularly-symmetric complex Gaussian noise with variance N_0 per complex entry. The channel matrix has the following block structure,

$$\mathbf{H} = \begin{bmatrix} \mathbf{H}_{1,1} & \cdots & \mathbf{H}_{1,K} \\ \vdots & & \vdots \\ \mathbf{H}_{L,1} & \cdots & \mathbf{H}_{L,K} \end{bmatrix}, \tag{2}$$

[1] This is not unrealistic since the APs consist of only few (e.g., four) antennas.
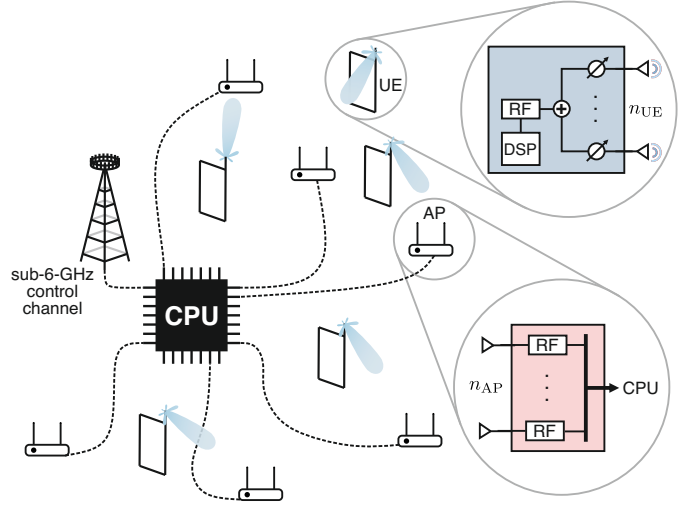

Fig. 1. Visualization of the considered cell-free scenario. The UEs use a single RF chain to load the antennas via phase shifters. The APs are fully digital [19].

where $\mathbf{H}_{\ell,k} \in \mathbb{C}^{n_{\mathrm{AP}} \times n_{\mathrm{UE}}}$ is the channel matrix from the kth UE to the ℓth AP. We use $\mathbf{H}_k = [\mathbf{H}_{1,k}^T, \ldots, \mathbf{H}_{L,k}^T]^T \in \mathbb{C}^{N_R \times n_{\mathrm{UE}}}$ to denote the kth column block of $\mathbf{H}$. Any effects of power control are absorbed into the channel matrix. The UE beamforming matrix $\mathbf{P}$ is block-diagonal, $\mathbf{P} = \mathrm{diag}(\mathbf{p}_1, \ldots, \mathbf{p}_K)$, with diagonal blocks $\mathbf{p}_k \in \mathbb{C}^{n_{\mathrm{UE}}}, k = 1, \ldots, K$. The block-diagonal structure reflects the fact that the UEs cannot transmit cooperatively. We assume UEs with a single RF chain and analog phase shifters, so that the codebook of possible beams is

$$\mathcal{P} = \left\{ \mathbf{p}(\phi_b) = \frac{1}{\sqrt{n_{\mathrm{UE}}}}[1, e^{-j\pi\cos\phi_b}, \ldots, e^{-j(n_{\mathrm{UE}}-1)\pi\cos\phi_b}]^T, \right.$$
$$\left. \phi_b \in \left\{ 0, \frac{\pi}{B}, \ldots, \frac{B-1}{B}\pi \right\} \right\}, \tag{3}$$

where $|\mathcal{P}| = B$ is the codebook size. Note that, since we use analog beamforming, the beamforming matrix $\mathbf{P}$ is identical for all subcarriers.

As in [16], we assume the existence of a sub-6-GHz control channel which can be used for control signaling from the CPU to the UEs. However, compared to [16], our scheme requires significantly less control signaling overhead: It only requires the CPU to communicate to each UE the codebook index of its selected beam and requires no control signals from the UEs.

A. Communication Scheme

MU interference-aware BA requires knowledge of the channel matrix in (2) or some surrogate thereof. Knowledge of the channel matrix in wireless systems is typically acquired through the transmission of pilots, which leads to a chicken-or-egg problem: On one hand, if the UEs transmit pilot symbols without using appropriate beamforming vectors, the APs will only pick up a very weak signal which does not allow reliable

CHEST.[2] On the other hand, some knowledge of the channel matrix is necessary for the UEs to select appropriate beams.

We solve this conundrum using a two-stage scheme: In the first stage, the UEs transmit non-orthogonal pilots in different directions to ensure sufficient receive signal strength for at least some of the directions. Based on these pilots, the CPU then performs a coarse estimate of the channel matrix which it then uses for BA. Note that this estimate of the channel matrix only needs to be accurate enough to determine the angles of strong receptivity. In the second stage, the UEs fix their beamformers to the selected beams, which are communicated to them via the available sub-6-GHz control channel. The UEs transmit orthogonal pilot sequences used by the CPU to perform a high-quality estimate of the compound of the channel matrix and the beamforming matrix $\mathbf{HP}$. This estimate is then used for data detection, which in this paper is performed using centralized LMMSE equalization $\hat{\mathbf{s}} = \mathbf{W}^H \mathbf{y}$ with

$$\mathbf{W} = \mathbf{HP}\left((\mathbf{HP})^H \mathbf{HP} + \frac{N_0}{E_s}\mathbf{I}_K\right)^{-1}. \qquad (4)$$

Many other detection methods, including decentralized ones, would of course be possible and are left for future work.

We will now first describe the BA procedure before explaining the pre-beam-alignment (pre-BA) and post-beam-alignment (post-BA) CHEST steps that precede and follow it, respectively.

III. BEAM ALIGNMENT

As stated in Section II-A, BA requires knowledge of the channel matrix (or some suitable surrogate thereof). It is important to remember that here we consider frequency-selective mmWave channels that can be divided into frequency-flat subcarriers. Ideally, BA would be applied to each of the subcarriers independently. However, since the UEs use analog beamforming, they can only form a single beam, which is then used for all subcarriers. We therefore perform BA based on the strongest subcarrier channel matrices per UE and AP, i.e., based on a surrogate matrix $\bar{\mathbf{H}} \in \mathbb{C}^{N_R \times N_T}$ consisting of the blocks $\bar{\mathbf{H}}_{\ell,k} = \arg \max_{v=1,\ldots,n_{sc}} \|\mathbf{H}^v_{\ell,k}\|^2_F$, where v is the subcarrier index.

Even when using such a frequency-flat surrogate, optimal BA is typically not practical for common optimization objectives such as achievable sum-rate or max-min achievable rate since it requires the optimization over a combinatorial set. For instance, for max-min achievable rate optimal BA, we would be required to solve the following optimization problem:

$$\max_{(\mathbf{p}_1,\ldots,\mathbf{p}_K) \in \mathcal{P}^K} \min_{k=1,\ldots,K} SINR_k(\mathbf{p}_1,\ldots,\mathbf{p}_K), \qquad (5)$$

where $SINR_k(\mathbf{p}_1,\ldots,\mathbf{p}_K)$ is the post-equalization signal-to-interference-plus-noise ratio (SINR) of the kth UE given the beamforming vectors $\mathbf{p}_1,\ldots,\mathbf{p}_K$:

$$SINR_k(\mathbf{p}_1,\ldots,\mathbf{p}_K) = \frac{|\mathbf{w}^H_k \mathbf{H}_k \mathbf{p}_k|^2}{\sum_{k' \neq k} |\mathbf{w}^H_k \mathbf{H}_{k'} \mathbf{p}_{k'}|^2 + N_0 \|\mathbf{w}_k\|^2_2}, \qquad (6)$$

[2]Because of channel reciprocity, the same would also hold if the pilots were transmitted by the APs instead of the UEs.

with $\mathbf{w}_k$ being the kth column of (4). Solving this optimization problem through an exhaustive search for $K = 32$ UEs and a codebook size of $B = 16$ would amount to $B^K \approx 10^{38}$ evaluations of the objective in (5). Clearly, this is not feasible in practice. We therefore now outline some more practical methods for BA.

A. Interference-Unaware Digital Beam Alignment

We start by discussing the well-known eigenbeamforming method [20], which in our case is not applicable because it would require digital beamforming, but which we will later use as a performance baseline. If MU interference were negligible (and the UEs could perform full digital beamforming), one could simply optimize the (pre-equalization) signal-to-noise ratio (SNR) for every user, by solving

$$\max_{\mathbf{p}} \frac{E_s \|\mathbf{H}_k \mathbf{p}\|^2_2}{N_R N_0} \text{ s.t. } \|\mathbf{p}\|_2 = 1, \ k = 1,\ldots,K, \qquad (7)$$

which yields the leading (= belonging to the largest singular value) right-singular vector of the per-UE channel matrix $\mathbf{H}_k$.

B. Interference-Unaware Analog Beam Alignment

In the considered scenario, the UEs can only form beams from the finite set (3) and so in general will be unable to beamform the leading right-singular vector of $\mathbf{H}_k$. However, if MU interference is negligible or ignored, we can still solve (7) to maximize the (pre-equalization) SNR for every UE, except that we now optimize over the codebook of possible beams $\mathcal{P}$ instead of the set $\{\mathbf{p} : \|\mathbf{p}\|_2 = 1\}$. Since this optimization problem can be solved individually per UE, we can solve it using an exhaustive search over KB possibilities.

C. Interference-Aware Analog Beam Alignment

As we will see in the Section V, ignoring MU interference results in suboptimal performance. For this reason, our proposed BA algorithm takes MU interference into account. We have already seen that maximizing joint optimization objectives, such as max-min-optimal achievable rate is impractical. For this reason, we use an algorithm in which the UEs greedily optimize their individual post-equalization SINR, given the currently selected beams of the other UEs. Such an algorithm can be succinctly motivated by a German idiom:[3] "When everyone thinks of themselves, everyone is taken care of." The method operates as follows: First, we perform a singular value decomposition (SVD) for each per-UE channel matrix $\mathbf{H}_k$, $k = 1,\ldots,K$. We then sort the UEs in descending order according to the largest singular value σ_k of their per-UE channel matrix $\mathbf{H}_k$. Assume now that the UEs are ordered in this way, i.e., $\sigma_k \geq \sigma_i$ for $i > k$. Starting from an empty set of UEs, we then iteratively select the beam for the kth UE which maximizes the post-equalization SINR, where the interference-term only takes into account the interference of those UEs whose beams have already been selected:

$$\mathbf{p}_k = \arg \max_{\tilde{\mathbf{p}}_k} \frac{|\mathbf{v}^H_k \mathbf{H}_k \tilde{\mathbf{p}}_k|^2}{\sum_{k' < k} |\mathbf{v}^H_k \mathbf{H}_{k'} \mathbf{p}_{k'}|^2 + N_0 \|\mathbf{v}_k\|^2_2}, \qquad (8)$$

[3]"Wenn jeder an sich denkt, ist an alle gedacht."

for $k = 1, \ldots, K$. In (8), $\mathbf{v}_k$ is the kth column of the LMMSE equalization matrix as in (4), but restricted to only the first k UEs, i.e., to those UEs whose beam has already been selected or is currently being selected. This means that $\mathbf{v}_k$ is a function of $\mathbf{p}_1, \ldots, \mathbf{p}_{k-1}$ and $\tilde{\mathbf{p}}_k$, as well as $\mathbf{H}_1, \ldots, \mathbf{H}_k$.

Then, in a second round, we use a coordinate descent approach where every UE has the chance to re-adjust its beams to adapt to the beams of the UEs that were selected later by taking into account the interference of *all* UEs according to their currently selected beams. This round iterates in reverse order, $k = K, \ldots, 1$,

$$\mathbf{p}_k = \arg\max_{\tilde{\mathbf{p}}_k} \frac{|\mathbf{v}_k^H \mathbf{H}_k \tilde{\mathbf{p}}_k|^2}{\sum_{k' \neq k} |\mathbf{v}_k^H \mathbf{H}_{k'} \mathbf{p}_{k'}|^2 + N_0 \|\mathbf{v}_k\|_2^2}, \quad (9)$$

where $\mathbf{v}_k$ now denotes the kth column of the LMMSE equalization matrix (4) considering *all* UEs, i.e., $\mathbf{v}_k$ is now a function of $\mathbf{p}_1, \ldots, \tilde{\mathbf{p}}_k, \ldots, \mathbf{p}_K$, as well as $\mathbf{H}_1, \ldots, \mathbf{H}_K$.

IV. CHANNEL ESTIMATION

The previous section on BA assumed that the channel matrix $\mathbf{H}$ is known for every subcarrier. We now describe our proposed method to estimate the channel with sufficient accuracy for the BA procedure.

A. Pre-Beam-Alignment Channel Estimation (Pre-BA CHEST)

To perform BA based on the strongest subcarrier, we would in principle have to estimate the channel matrix for every subcarrier individually. However, to keep complexity at bay, and since large-scale fading properties do not change dramatically between adjacent subcarriers, we only estimate the channel matrix for a subset of subcarriers which are spaced uniformly over the total number of used subcarriers.

We now describe the CHEST in per-subcarrier fashion, where we again omit the subcarrier index for brevity. We estimate the channel matrix at the APs using pilot signals transmitted from the UEs for n_{pilot} time slots, i.e., we observe

$$\mathbf{Y} = \mathbf{HB} + \mathbf{N}, \quad (10)$$

where the matrix $\mathbf{B} \in \mathbb{C}^{N_T \times n_{pilot}}$ is the compound of the UE transmit symbols and the beams they form while transmitting them. Assuming that the matrix $\mathbf{B}$ (which we call the beam-pilot matrix) is known, the APs estimate $\mathbf{H} \in \mathbb{C}^{N_R \times N_T}$ based on $\mathbf{Y} \in \mathbb{C}^{N_R \times n_{pilot}}$. Note that, since this happens before the BA phase, the beams which can be used by the UEs in $\mathbf{B}$ need to be predetermined. To explore the channels' characteristics as fully as possible and to make sure that we get adequate signal receive power at least during some of the time slots of $\mathbf{Y}$, the UEs essentially sweep through the beam codebook. The kth UE transmits the per-UE beam-pilot matrix $\mathbf{B}_{(k,\cdot)} \in \mathbb{C}^{n_{UE} \times n_{pilot}}$, which is the kth row block of $\mathbf{B}$ and whose columns contain all beams $\mathbf{p} \in \mathcal{P}$.[4] If all of the UEs would transmit their beam pilots simultaneously, we would have the most efficient CHEST scheme with $n_{pilot} = B$. However, depending on the number of UEs K and the size of the beam codebook B, the matrix $\mathbf{B}$

[4]This means that the UE pilot symbols for the pre-BA CHEST are all 1.

can become very tall, which results in degenerate estimates of the channel matrix $\mathbf{H}$. Conversely, if only one UE at a time transmits its pilot beams, CHEST is much easier but the scheme becomes time consuming, with $n_{pilot} = BK$ time slots.

To develop a scheme which is both sufficiently accurate and efficient, we use a clustering scheme, where the K UEs are randomly clustered into C equisized clusters: All UEs belonging to the same cluster transmit their pilot beams simultaneously, while the different clusters transmit their pilot beams sequentially, resulting in $n_{pilot} = BC$.

We also use an informative prior that exploits the block sparsity of the channel matrix $\mathbf{H}$ which results from the distributed nature of the APs and the UEs in combination with the high directivity of mmWave channels [1]. Specifically, we estimate $\mathbf{H}$ by solving the convex optimization problem

$$\hat{\mathbf{H}} = \arg\min_{\mathbf{H} \in \mathbb{C}^{N_R \times N_T}} \frac{1}{2} \|\mathbf{Y} - \mathbf{HB}\|_F^2 + \mu \|\mathbf{H}\|_{BS}, \quad (11)$$

where μ is a regularization parameter and where we use the block sparsity promoting prior [21]

$$\|\mathbf{H}\|_{BS} = \sum_{\ell=1}^{L} \sum_{k=1}^{K} \|\mathbf{H}_{\ell,k}\|_F. \quad (12)$$

The optimization problem (11) can be efficiently solved using forward-backward-splitting (FBS) [22].

B. Post-Beam-Alignment Channel Estimation (Post-BA CHEST)

Using the estimates $\hat{\mathbf{H}}$ in (11) of the channel matrices for the different subcarriers, the CPU then performs BA as detailed in Section III and communicates the selected beams to the UEs using the sub-6-GHz control channels. The UEs then fix their beams accordingly in the form of the beamforming matrix $\mathbf{P}$. With these beams now being fixed, we effectively have a compound channel matrix $\mathbf{HP} \in \mathbb{C}^{N_R \times K}$ for every subcarrier. Since the beams $\mathbf{P}$ have been appropriately selected, we can estimate this compound channel (for *every* subcarrier) with high accuracy for reliable data detection. We do this by letting the UEs transmit pilot sequences which together form a Hadamard matrix. The APs then estimate $\mathbf{HP}$ using least squares estimation.

V. NUMERICAL RESULTS

We now evaluate the performance of our proposed scheme in comparison with a number of baselines.

A. Simulation Setup

We simulate a local cell-free communication scenario in which $K = 32$ UEs, each with $n_{UE} = 8$ antennas, communicate with $L = 16$ APs, each with $n_{AP} = 4$ antennas. We use a carrier frequency of 28 GHz and a bandwidth of 1 GHz divided into $n_{sc} = 2048$ orthogonal subcarriers. For the pre-BA CHEST procedure, we estimate the channels of the subcarrier indices $v \in \{1, 229, 456, 684, 911, 1139, 1366, 1594, 1821, 2048\}$ and considering $C = 8$ equisized clusters. The BA step is performed based on the strongest subcarrier channel matrices per UE and AP, as detailed in Section III. The UEs use a
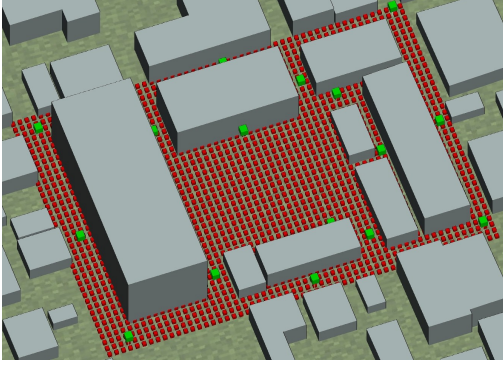
Fig. 2. Simulated scenario with 1336 possible UE locations (red), each with $n_{\mathrm{UE}} = 8$ antennas, and $L = 16$ APs (green), each with $n_{\mathrm{AP}} = 4$ antennas.

QPSK transmit constellation and transmit at a maximum power of $20\,\mathrm{dBm}$ using $\pm 3\mathrm{dB}$ power control. To model realistic RF hardware, the APs have a noise figure of $7\,\mathrm{dB}$ [23].

The wireless channels are simulated using Wireless InSite from Remcom [18]. The setup, depicted in Fig. 2, consists of a $200\,\mathrm{m} \times 280\,\mathrm{m}$ area and contains 1336 possible UE locations (visualized in Fig. 2 as red squares) which are arranged on a grid. To simulate random user orientations, we also consider four possible angles for each user: $\{0°, 45°, 90°, 135°\}$. The position and orientation of the APs are fixed. The APs and UEs are at heights of $12\,\mathrm{m}$ and $1.65\,\mathrm{m}$, respectively. Both APs and UEs have uniform linear arrays with omnidirectional antennas spaced by half a wavelength.

B. Performance Metrics and Baseline Methods

As performance metrics we consider the cumulative density function (CDF) or complementary CDF (CCDF) of the root-mean-squared-symbol error (RMSSE) per UE, the SINR per UE per subcarrier, and the spectral efficiency (SE) per UE (summed over all subcarriers), all considering an LMMSE equalizer. The RMSSE for the kth UE is defined as

$$RMSSE_k = \sqrt{\frac{\sum_{v=1}^{n_{\mathrm{sc}}} \sum_{t=1}^{T_D} \left| \hat{s}_k^{(tv)} - s_k^{(tv)} \right|^2}{\sum_{v=1}^{n_{\mathrm{sc}}} \sum_{t=1}^{T_D} \left| s_k^{(tv)} \right|^2}}, \qquad (13)$$

where T_D is the number of time slots and $\hat{s}_k^{(tv)}$ and $s_k^{(tv)}$ are the estimated and transmitted symbols of the kth UE in the vth subcarrier in the tth time slot, respectively.

In our numerical results, we refer to the interference-unaware analog BA from Section III-B as "analog IU" and to the interference-aware analog BA from Section III-C as "analog IA." As the first baseline method, we use "single antenna," where each UE has $n_{\mathrm{UE}} = 1$ antenna, i.e., no BA capabilities. For a fair comparison, the total transmit power of "single antenna" UEs is the same as for the multi-antenna techniques. The second baseline is the interference-unaware digital BA from Section III-A, which we refer to as "digital IU."

C. Performance Results

Fig. 3 shows BA results which consider ground-truth channel knowledge; Fig. 4 shows results where no such knowledge is

available and hence we estimate the channel as described in Section IV. To prove the efficacy of our proposed pre-BA CHEST scheme from Section IV-A, Fig. 3 also contains results where we combine pre-BA CHEST for BA with ground truth channel knowledge for data equalization (dashed curves). The fact that the results where we perform pre-BA CHEST are virtually identical to the results where perfect channel knowledge is available also for the BA step proves that our pre-BA CHEST procedure solves its task nearly optimally. Any performance deterioration from Fig. 3 to Fig. 4 is due to the loss incurred by the post-BA CHEST for data detection, where we only used a plain vanilla least squares channel estimator.

The performance hierarchy between the methods is very similar for all performance metrics, and regardless of whether channel knowledge is available or has to be estimated. The "single-antenna" method has the worst performance among all considered approaches. This shows that omnidirectional single-antenna UEs suffer from significant performance losses in cell-free mmWave systems compared to beamforming-capable UEs with adequately selected beams. The "digital IU" method and its analog counterpart "analog IU" perform substantially better. Notably, "analog IU" is almost as good as "digital IU," suggesting that the more limited expressiveness of the beams that can be formed by the "analog IU" compared to "digital IU" are not negatively affecting the performance. Finally, the "analog IA" achieves by far the best performance. The difference between "analog IA" and the interference-unaware methods is larger for the weakest UEs. The spectral efficiency of the 10% weakest UEs is essentially $1.3\times$ better for the interference-aware method than for the interference-unaware methods. This shows that optimal BA of dense cell-free mmWave networks requires algorithms that select the beams for the UEs jointly and take MU interference into account. Contrastingly, the precise RF architecture and resulting beamforming expressivity of the UEs seem to be comparably less important.

VI. CONCLUSIONS

We have proposed an interference-aware beam alignment method together with a channel estimation scheme for cell-free mmWave massive MU-MIMO systems. Our results have shown that multi-user interference-aware beam alignment consistently outperforms methods that do not take multi-user interference into account, which in turn outclass omnidirectional transmission without beamforming. We have also shown the efficacy of our proposed pre-beam-alignment channel estimation method in comparison to a hypothetical scenario where ground truth channel knowledge is available. For future work we highlight the combination of our methods with decentralized data detection schemes as well as considering the UE beam alignment problem in the mmWave cell-free downlink.

REFERENCES

[1] T. S. Rappaport, S. Sun, R. Mayzus, H. Zhao, Y. Azar, K. Wang, G. N. Wong, J. K. Schulz, M. Samimi, and F. Gutierrez, "Millimeter wave mobile communications for 5G cellular: It will work!" *IEEE Access*, vol. 1, pp. 335–349, May 2013.
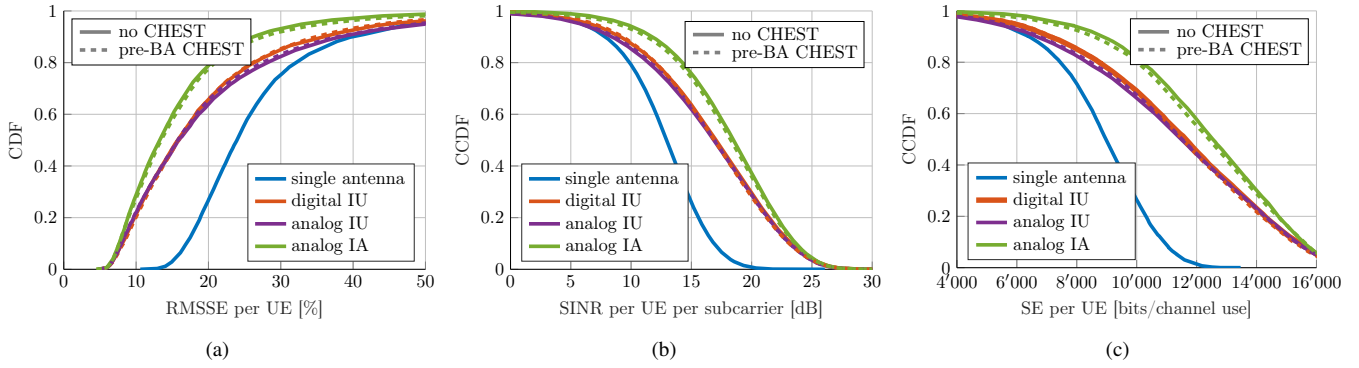
Fig. 3. Subfigures (a), (b), and (c) show the CDF or CCDF of the RMSSE per UE, the SINR per UE per subcarrier, and the SE per UE, respectively, for ground truth channel knowledge (solid) or pre-BA CHEST in combination with perfect post-BA CHEST (dashed).
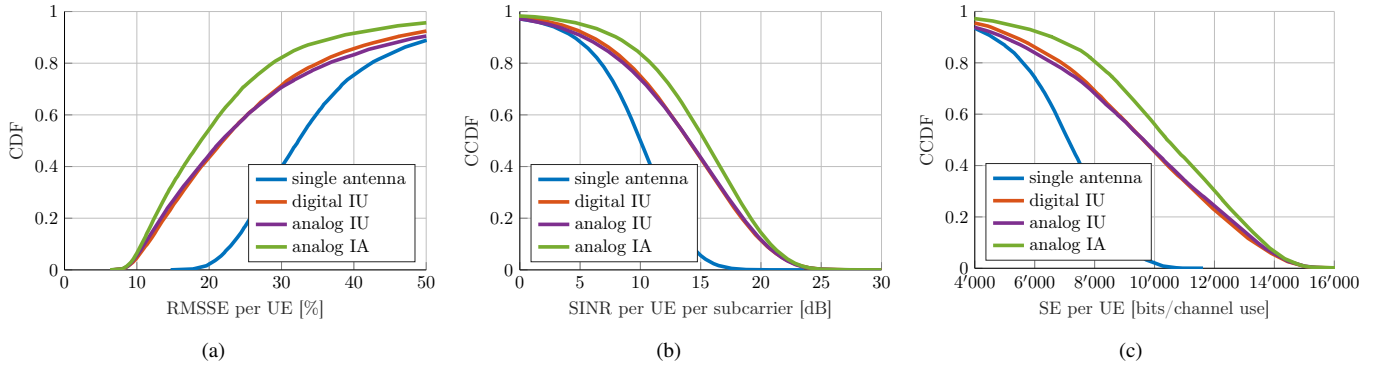

Fig. 4. Subfigures (a), (b), and (c) show the CDF or CCDF of the RMSSE per UE, the SINR per UE per subcarrier, and the SE per UE, respectively, in the absence of ground truth channel knowledge, i.e., using both pre-BA and post-BA CHEST.

[2] M. Alonzo and S. Buzzi, "Cell-free and user-centric massive MIMO at millimeter wave frequencies," in *Proc. IEEE Ann. Int. Symp. Personal, Indoor, and Mobile Radio Commun. (PIMRC)*, Oct. 2017, pp. 1–5.

[3] R. W. Heath, N. Gonzalez-Prelcic, S. Rangan, W. Roh, and A. M. Sayeed, "An overview of signal processing techniques for millimeter wave MIMO systems," *IEEE J. Sel. Topics Signal Process.*, vol. 10, no. 3, pp. 436–453, Apr. 2016.

[4] M. Xiao, S. Mumtaz, Y. Huang, L. Dai, Y. Li, M. Matthaiou, G. K. Karagiannidis, E. Björnson, K. Yang, I. Chih-Lin *et al.*, "Millimeter wave communications for future mobile networks," *IEEE J. Sel. Areas Commun.*, vol. 35, no. 9, pp. 1909–1935, Sep. 2017.

[5] Apple Inc., "iPhone 13," https://www.apple.com/iphone-13/specs/, Accessed: 2022-04-06.

[6] H. Q. Ngo, A. Ashikhmin, H. Yang, E. G. Larsson, and T. L. Marzetta, "Cell-free massive MIMO versus small cells," *IEEE Trans. Wireless Commun.*, vol. 16, no. 3, pp. 1834–1850, Mar. 2017.

[7] G. Interdonato, E. Björnson, H. Quoc Ngo, P. Frenger, and E. G. Larsson, "Ubiquitous cell-free massive MIMO communications," *EURASIP J. Wireless Commun. Netw.*, vol. 2019, no. 1, pp. 1–13, Aug. 2019.

[8] S. Buzzi and C. D'Andrea, "Cell-free massive MIMO: User-centric approach," *IEEE Wireless Commun. Lett.*, vol. 6, no. 6, pp. 706–709, Dec. 2017.

[9] S. Kim and B. Shim, "Energy-efficient millimeter-wave cell-free systems under limited feedback," *IEEE Trans. Commun.*, vol. 69, no. 6, pp. 4067–4082, Jun. 2021.

[10] J. Wang, B. Wang, J. Fang, and H. Li, "Millimeter wave cell-free massive MIMO systems: Joint beamforming and AP-user association," *IEEE Wireless Commun. Lett.*, Feb. 2021.

[11] G. Femenias and F. Riera-Palou, "Cell-free millimeter-wave massive MIMO systems with limited fronthaul capacity," *IEEE Access*, vol. 7, pp. 44 596–44 612, 2019.

[12] J.-C. Guo, Q.-Y. Yu, W.-B. Sun, and W.-X. Meng, "Robust efficient hybrid pre-coding scheme for mmWave cell-free and user-centric massive MIMO communications," *IEEE Trans. Wireless Commun.*, vol. 20, no. 12, pp. 8006–8022, Dec. 2021.

[13] Q. Xue, Q. Li, C. Dong, S. Suo, and K. Niu, "Beam selection for cell-free millimeter-wave massive MIMO systems," in *Proc. IEEE Asia-Pacific Conf. Commun. (APCC)*, Oct. 2021, pp. 310–315.

[14] C. M. Yetis, E. Björnson, and P. Giselsson, "Joint analog beam selection and digital beamforming in millimeter wave cell-free massive MIMO systems," *IEEE Open J. Commun. Soc.*, vol. 2, pp. 1647–1662, 2021.

[15] M. Alonzo, S. Buzzi, A. Zappone, and C. D'Elia, "Energy-efficient power control in cell-free and user-centric massive MIMO at millimeter wave," *IEEE Trans. Green Commun. Netw.*, vol. 3, no. 3, pp. 651–663, Sep. 2019.

[16] S. Buzzi, C. D'Andrea, M. Fresia, and X. Wu, "Beam alignment in mmWave user-centric cell-free massive MIMO systems," in *Proc. IEEE Global Commun. Conf. (GLOBECOM)*, Dec. 2021, pp. 1–6.

[17] H. Song, T. Goldstein, X. You, C. Zhang, O. Tirkkonen, and C. Studer, "Joint channel estimation and data detection in cell-free massive MU-MIMO systems," *IEEE Trans. Wireless Commun.*, pp. 1–17, 2021.

[18] Remcom, "Wireless InSite," https://www.remcom.com/wireless-insite-em-propagation-software, Accessed: 2022-04-06.

[19] E. Björnson and L. Sanguinetti, "Making cell-free massive MIMO competitive with MMSE processing and centralized implementation," *IEEE Trans. Wireless Commun.*, vol. 19, no. 1, pp. 77–90, Jan. 2020.

[20] D. Tse and P. Viswanath, *Fundamentals of wireless communication*. Cambridge Univ. Press, 2005.

[21] S. F. Cotter, B. D. Rao, K. Engan, and K. Kreutz-Delgado, "Sparse solutions to linear inverse problems with multiple measurement vectors," *IEEE Trans. Signal Process.*, vol. 53, no. 7, pp. 2477–2488, Jul. 2005.

[22] T. Goldstein, C. Studer, and R. G. Baraniuk, "A field guide to forward-backward splitting with a FASTA implementation," *arXiv*, vol. abs/1411.3406, 2014. [Online]. Available: http://arxiv.org/abs/1411.3406

[23] R. Lu, C. Weston, D. Weyer, F. Buhler, and M. P. Flynn, "A 16-element fully integrated 28GHz digital beamformer with in-package 4×4 patch antenna array and 64 continuous-time band-pass delta-sigma sub-ADCs," in *Proc. IEEE Radio Freq. Integr. Circuits Symp. (RFIC)*, Aug. 2020, pp. 343–346.